Vladimir Krasnov

Experimental Condensed Matter Physics Group
Fysikum, AlbaNova, Stockholm University

Natural Atomic Superlattices: Physics and Applications

- Who we are
- Research directions
- Superlattices artificial and natural
- Intrinsic Josephson effect in $Bi_2Sr_2CaCu_2O_8$
- Intrinsic tunneling spectroscopy
- Possible applications
- **Conclusions**

Instrumentation seminar, 17 November 2005, AlbaNova

Experimentell Kondenserade Materiens Fysik

Historien:

V.K. = Vladimir Krasnov (Professor)
T.G. = Taras Golod (Doktorand)
A.E. = Arvin Emadi (Doktorand)
A.R. = Andeas Rydh (Forskarassistent)

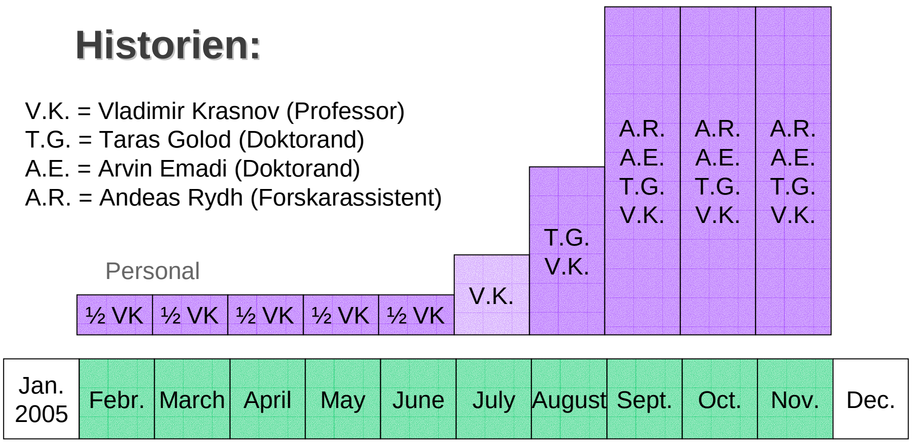

17 November 2005, Fysikum, AlbaNova, Stockholms Universitet

Forskning inriktningar

• Naturliga atomära supergitter: Fysik och Tillämpningar
(V.Krasnov och A.Emadi)

- THz tillämpningar

- Intrinsisk tunnelspektroskopi av HTSC och andra material med lager struktur

• Hybrid Supraledare-Ferromagnet komponenter för kvantelektronik
(T.Golod och V.Krasnov)

• Nano-kalorimetri
(A.Rydh)

• Nanoteknologi

Dual-beam SEM / FIB

Focused Ion Beam

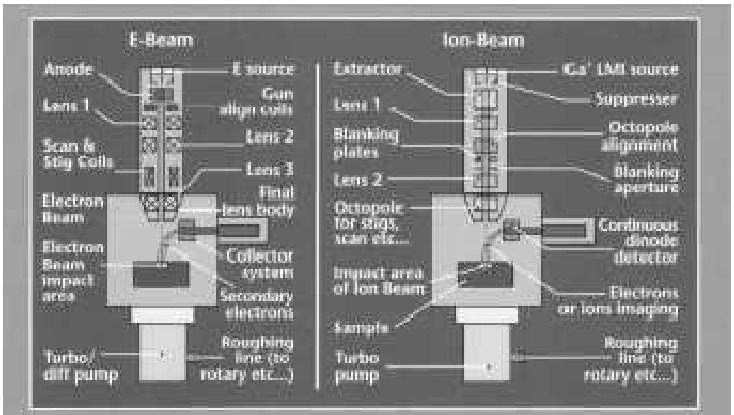

Figure 6: Schematic presentation of SEM and FIB and the many similarities of the instruments.

Focused Ion Beam

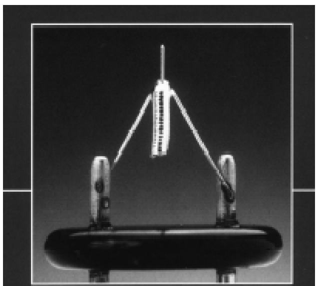

Figure 4: The Ga liquid metal ion source, including the reservoir.

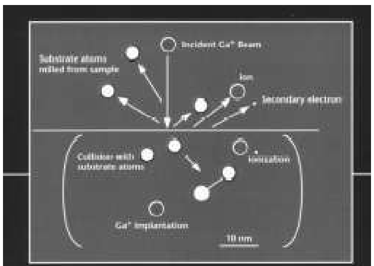

Figure 5: Interactions of the ion beam with the sample surface. The unique control offered by beam currents and spot sizes allow use of the FIB for both nano engineering as well as for high resolution imaging using secondary electrons as well as ions.

What it can do?

- Maskless patterning (spotsize ~5nm)
- Etching: Physical (Sputtering) and Physical-Chemical (CAIBE)
- Deposition of various materials (Ion-Beam Assisted CVD)
- 3D – sculpturing
- Characterization SEM + grain structure, mass spectroscopy
- Crossectioning
- Fix / repair

Nano-kalorimetri som instrument för mesoskopisk forskning

Andreas Rydh i samarbete med Argonne National Lab

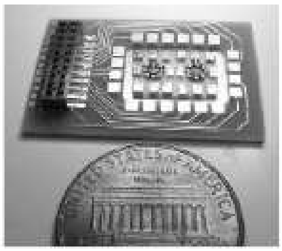

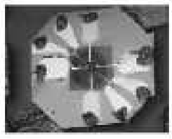

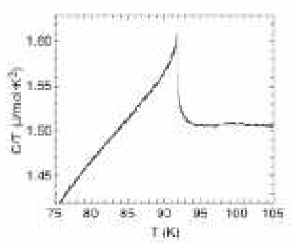

Huvuddrag:

MEMS-sensorer, ~ng upplösning

Nano-kalorimetri är ett avanserad forskning instrument som har även stora möjligheter till tillämpningar.

Fördelar med små prover:

- Den högsta kvalitet (t.ex. små monokristaller – viktig för utveckling av nya material).
- Några material finns bara I små mängder (t.ex. tynna filmer) eller svåra/dyra att produsera.
- Kvantmekaniska fenomen I mesoskopiska objekt kan studeras.
- Snaba fasövergångens dynamiken kan studeras (omöjligt för stora prover).

Forsknings ämnen:

(a) **Confinement effects in protein solutions** (protein folding, DNA base pair mismatch, and time dependence).

(b) **Kvant fasövergångar och kvant fluctuationer** (för att studera sk. “quantum criticality” fenomen).

(c) **Mesoskopisk supraledning** (kvantmekaniska tilstånd i mesoskopiska system)

Hybrid Supraledare-Ferromagnet Komponenter för Kvantelektronik

(Taras Golod och Vladimir Krasnov)

Syftet är att utveckla de nya supraledande kvant-komponenter för elektronik / spintronik

Fördel av S: makroskopisk fas-coherence som tillåter kvant fenomen på makroskopisk skala

- **Supraledande spintronik:** spin-polarizerat spridning av elektroner I S/F strukturer kan användas för nya spintronik komponenter
  - Absolut spin-ventil (100% spin-polarizerat)
  - Spin-SET (En Spin Transistor)
- **π-Josephson övergångar**, med spontant π-shift i fas, d.v.s. inverterat Josephson koppling, kan uppnås.
  - “fas-batterier” för kvantdatorer, som tillåter urkoppling från elektromagnetisk miljö och kan leda till s.k. tyst qubit (bas element i kvantdator)
  - komplementerande Josephson digitala kretsar.

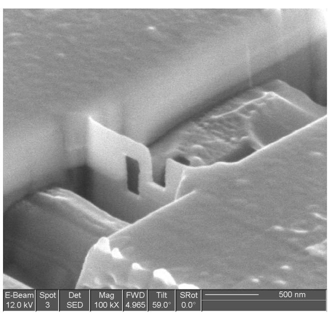

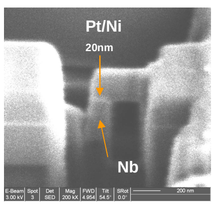

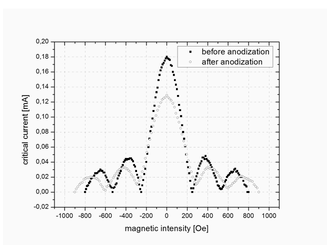

Cross-sectional STM of InAlAs/InGaAs quantum cascade laser

J.Faist, et al., Science 264 (1994) 553

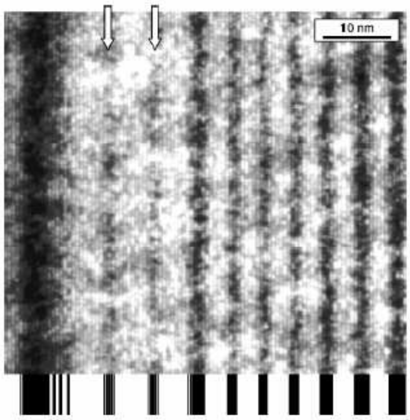

FIG. 1. 60×60 nm^2 filled states STM image of the graded structure with layer sequence indicated at the bottom of the image, $V_{sample} = -1.6$ V. The black layers are the InAlAs barriers and the white layers are the InGaAs wells.

P.Offermans et al., Appl.Phys.Lett. 83 (2003) 4131

Natural atomic superlattices in layered compounds

$Bi_2Sr_2CaCu_2O_{8+x}$: anisotropy ρ_c/ρ_{ab} ~10^6

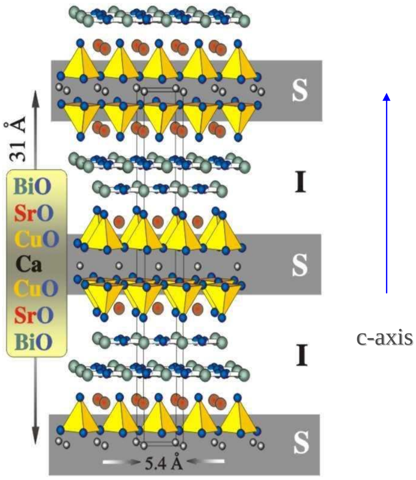

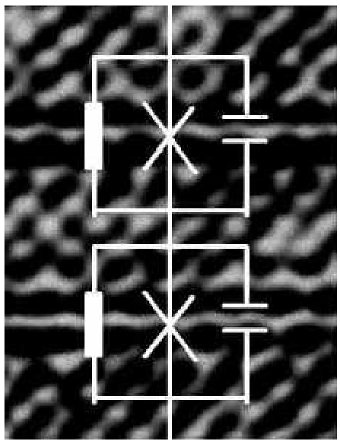

High-T_c superconductor -> Intrinsic Josephson effect at $T<T_c$

Evidences for tunneling nature of interlayer tunneling in layered compounds:

- Bi- and Tl-based cuprates ($Bi_2Sr_2CaCu_2O_8$, $Ta_2Ba_2Ca_2Cu_3O_{10}$, etc.)
- Transition metal halcogenides ($NbSe_3$, LaSe-$NbSe_2$, etc.)
- Organic conductors (k-$(BEDT\text{-}TTF)_2Cu(NCS)_2$, etc.)
- Manganites $La_{1.4}Sr_{1.6}Mn_2O_7$
- Magnetic superconductor $RuSr_2GdCu_2O_8$
- Intercalated compounds

Unusual physical properties due to low dimensional (2D or quasi-1D) electronic structure:

- Colossal magnetoresistance, magnetism
- Charge/Spin density waves
- High-Tc superconductivity

* Important for fundamental condensed matter physics

* Novel applications: Electronics/Spintronics at the ultimate atomic scale?

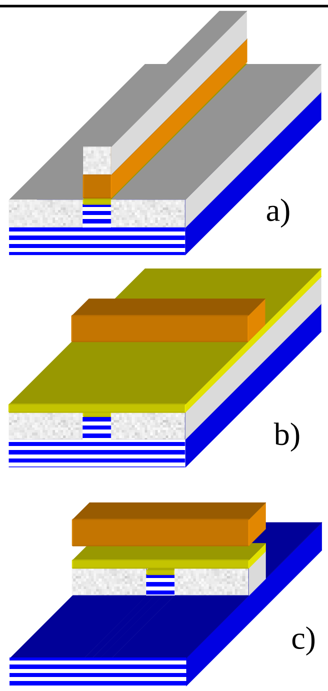

Sample fabrication:

1. Self-alignment Cross-bar Photolithography

Bi-2212 | **Au** | **CaF_2** | **Ph. Res.**

2. Trimming by Focused Ion Beam writing

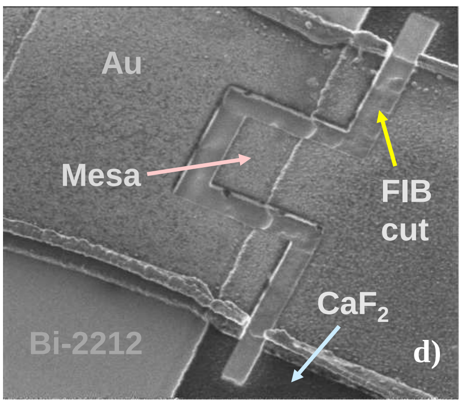

Multi-terminal devices

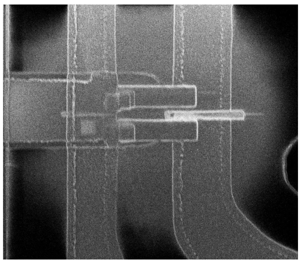

Cutting and deposition of extra contact electrodes (Pt) by FIB

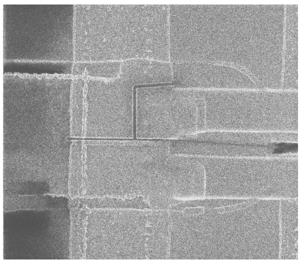

Cutting after deposition of Pt electrodes for true 4-probe measurements

DC Josephson Effect

$I_s = I_c \sin(\varphi)$.

Fraunhofer pattern

$$I_{\max} = I_c \left| \frac{\sin(\pi\Phi/\Phi_0)}{\pi\Phi/\Phi_0} \right|$$

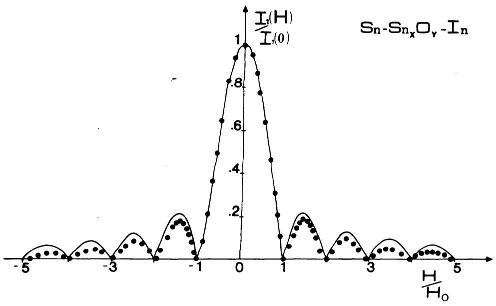

Evidence for DC- intrinsic Josephson effect

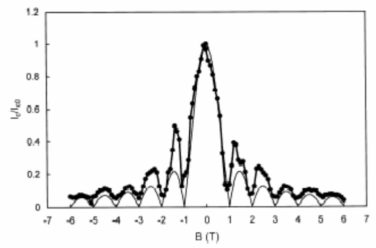

Fig. 2. Magnetic field B dependencies of critical currents of $Bi_2Sr_2CaCu_2O_8$ junctions at $T = 4.2$ K. B is parallel to the layers for the junction size of 1.5×1.5 μm^2 with a hole of $\Phi = 0.2$ μm.

From: T.Yamashita, et.al., Physica C 335 (2000) 219

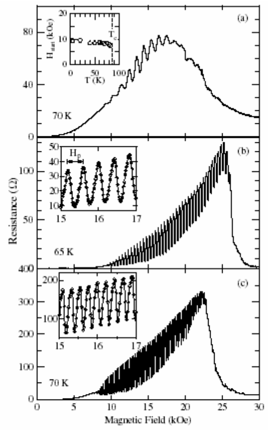

FIG. 2. Flow resistance of Josephson vortices as a function of magnetic field of samples *A* (a), *B* (b), and *C* (c) with an applied current of 1, 1, and 10 μA, respectively. The inset of (a) shows the temperature dependence of H_{start} for sample *B*. The enlarged figures of the flow-resistance oscillations of samples *B* and *C* are shown in the insets of (b) and (c), respectively.

From S.Ooi, et al., Phys.Rev.Lett. 89 (2002) 247002

Probing the intrinsic Josephson potential by thermal activation

Mechanical analog of RCSJ model - the tilted washboard potential

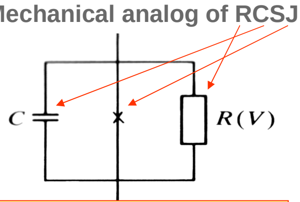

$$\frac{\partial^2 \varphi}{\partial \tau^2} + \frac{1}{Q}\frac{\partial \varphi}{\partial \tau} + \sin(\varphi) = \frac{I}{I_{c0}}$$

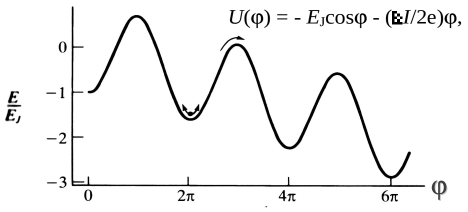

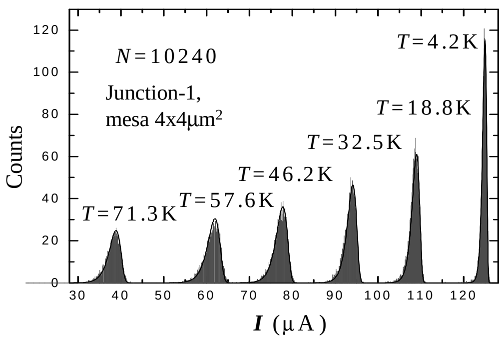

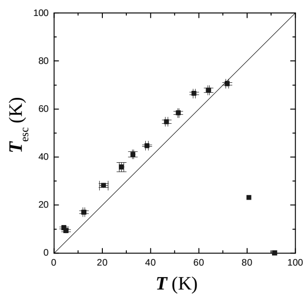

V.M.Krasnov, et al., Phys.Rev.B 72 (2005) 012512

AC Josephson Effect

$$\hbar\omega_J = 2eV$$

Resonance with external radiation, Shapiro steps.

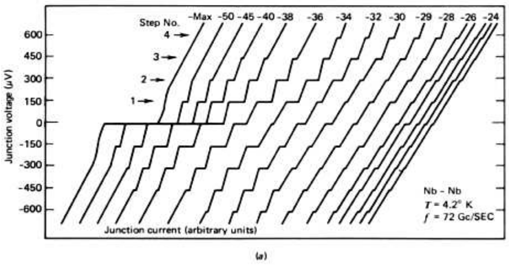

$$\omega_f = \frac{2e}{\hbar} V_0 = \pm n\omega_r$$

Geometrical resonances, Fiske steps

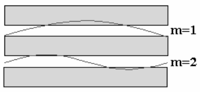

Standing waves in a transmission line

$$c_0 = 1\sqrt{LC} = c\sqrt{\frac{t}{\varepsilon_r d}}$$

Swihart velocity

$$V_n = \frac{\hbar}{2e}\omega_n = \frac{h}{2e}\frac{\bar{c}}{2L}n$$

AC intrinsic Josephson effect: **Fiske steps**

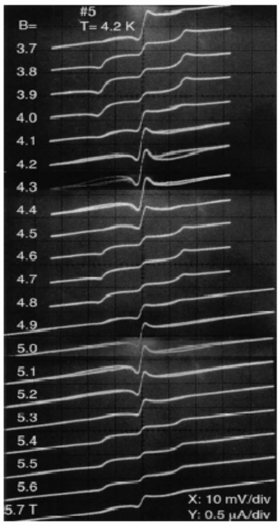

Fig. 7. A set of the I–V characteristics of a short Bi-2212 stack #5 with variation of parallel magnetic field $B_\parallel$ within 3.7–7.5 T, $T = 4.2$ K. Note a Fiske step at $V \approx 15$ mV.

Y.I. Latyshev, et al., Physica C 367 (2002) 365

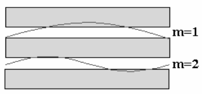

$$\Delta V_{FS} = N\frac{\Phi_0 c}{4L}\sqrt{\frac{td}{\varepsilon\lambda^2}} \cong 65\mu V$$

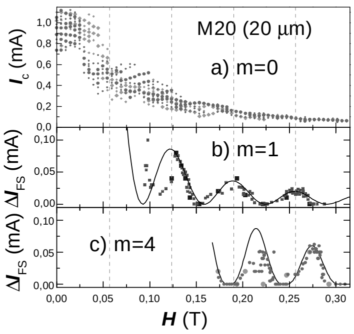

$$\Delta H = \frac{\Phi_0}{Ls} \Rightarrow s = 15.5\,\text{Å}$$

From: V.M.Krasnov, et al, PRB 59 (1999) 8463

AC – intrinsic Josephson effect : **Shapiro steps**

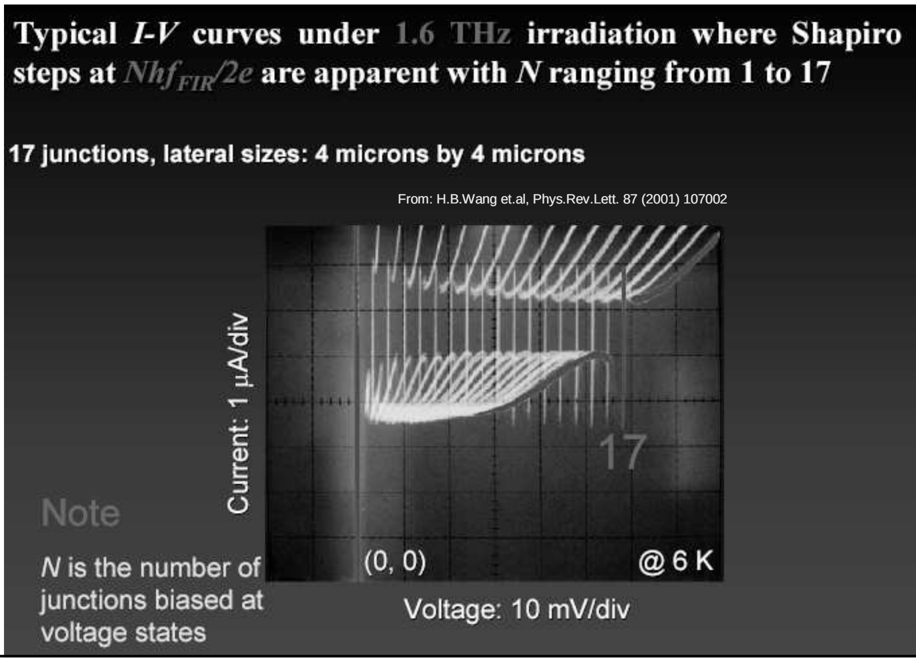

Conclusions-1

At present the existence of both AC and DC intrinsic Josephson effects are established in Bi-2212.

DC-Josephson effect:
- **Fraunhofer modulation of I_c**
- **Sinusoidal current-phase relation was probed by thermal activation from the wash-board potential**

AC-Josephson effect:
- **Shapiro steps**
- **Fiske steps**

2. Fluxon dynamics

Josephson vortices in a single Josephson junction

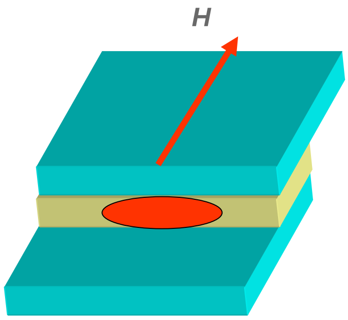

Static case:

$\varphi(x) = 4\arctan[\exp(x/\lambda_J)]$.

$\Phi = \Phi_0$ The "fluxon"

Dynamic case

Traveling Soliton $\varphi = \varphi(x - ut)$,

$\tilde{\lambda}_J \rightarrow \lambda_J \sqrt{1-(u/c_0)^2}$

Lorentz contraction of fluxon !

Special theory of relativity

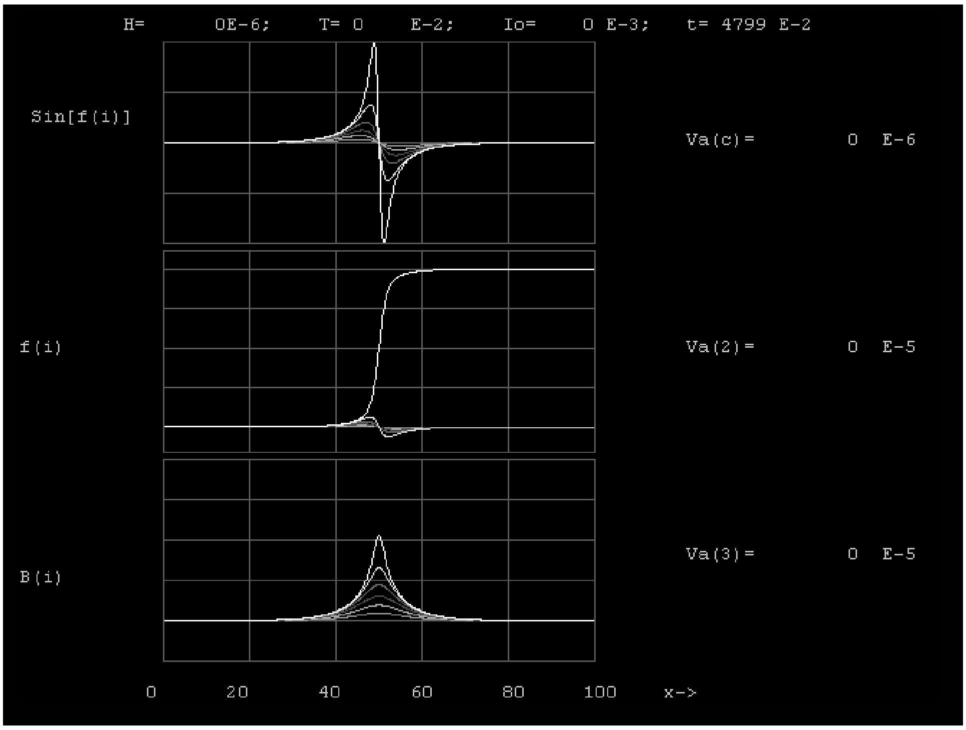

3. Intrinsic tunneling spectroscopy of HTSC

c-axis Current-Voltage characteristics of $Bi_2Sr_2CaCu_2O_{8+x}$ mesas

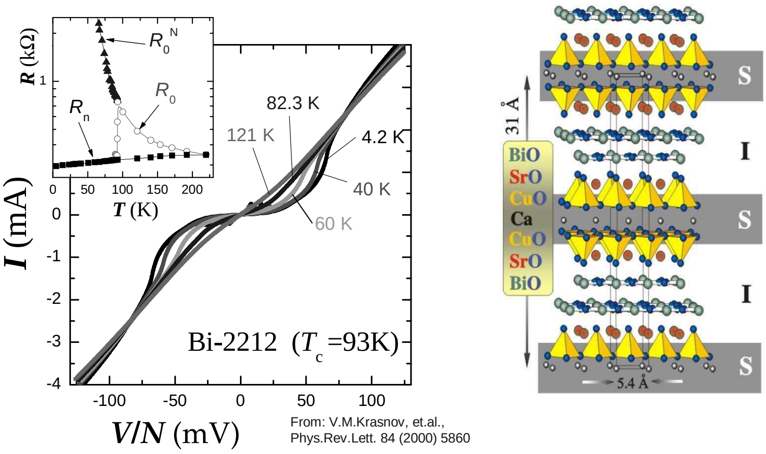

From: V.M.Krasnov, et.al., Phys.Rev.Lett. 84 (2000) 5860

I-V curves of small Bi2212 mesas exhibit typical SIS type tunnelling IVC's with almost T-independent normal resistance and a pronounced knee at the sum-gap voltage $V=2N\Delta/e$.
Inset shows *T*- dependencies of the zero bias R_0, normal R_N and the total sub-gap R_0^N resistances.

Intrinsic Tunnelling Spectroscopy – Unique way to probe BULK electronic properties of HTSC

Advantages of Intrinsic Tunneling Spectroscopy

1. ITS probes bulk properties and is insensitive to surface deterioration or surface states.
2. The current direction (c-axis) is well defined.
3. The tunnel barrier is atomically perfect and there are no "extrinsic" reasons for scattering during tunneling.
4. Mesa structures are mechanically stable and can be used for measurements at high bias in a wide range of temperatures and magnetic fields.

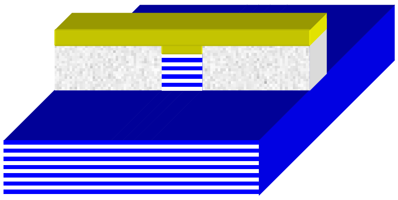

A sketch of a mesa structure on top of Bi-2212 single crystal

Smaller mesa size = better resolution.

*** Less defects** ($\propto a^2$): pure c-axis tunneling

*** Less self-heating** ($\propto a$):

V.M.Krasnov, et.al., J.Appl.Phys. 89 (2001) 5578, ibid. 93 (2003) 1329

Evidence for co-existence of the Superconducting- and the Pseudo-gaps

Optimally doped Bi-2212

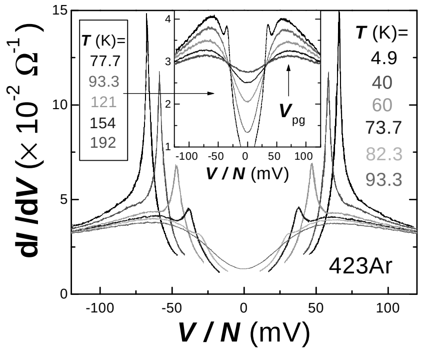

Dynamic conductance of a Bi2212 mesa at different *T*. Inset shows detailed curves for high T. Coexistence of the superconducting peak, V_S, and the pseudo-gap hump, V_{PG}, is clearly visible at *T*=77.7 K.

From: V.M.Krasnov, et.al., Phys.Rev.Lett. 84 (2000) 5860

Temperature dependence

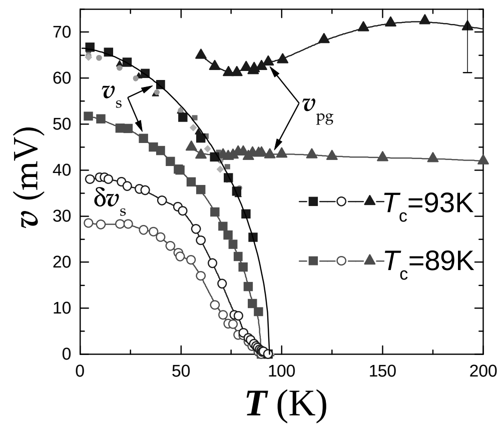

V.M.Krasnov, et.al., Phys.Rev.Lett. 84 (2000) 5860

Magnetic field dependence of the gaps

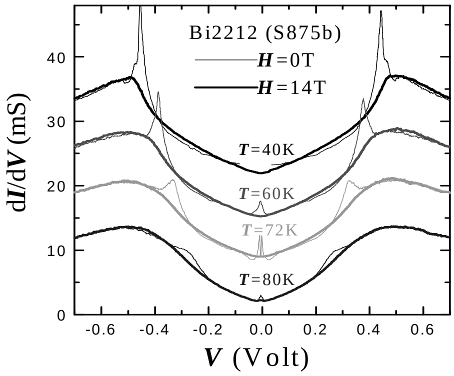

$\sigma(V)$ curves of a Bi2212 mesa at different T for H=0 (thin lines) and H=14T along the c-axis (thick lines) . The existence of a (T,H) dependent superconducting peak and the (T,H) independent "background" PG dip-and-hump is clearly seen.

From: V.M.Krasnov, et.al., Phys.Rev.Lett. 86 (2001) 2657

Phonon spectroscopy

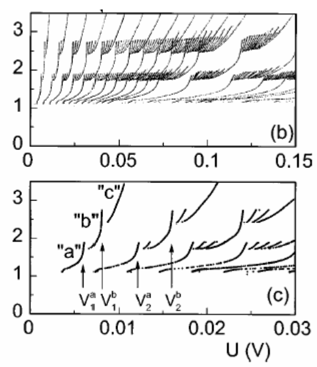

K.Schlenga, et al., Phys.Rev.B 57 (1998) 14518

$$2eV = \hbar\,\omega_{PhR}$$

Inelastic interaction between ac-Josephson effect and optical Raman active phonons

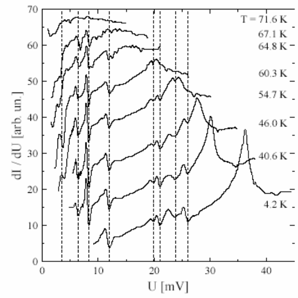

Fig. 4. Fine structure in the dI/dU-characteristics of a Josephson break junction in a BSCCO single crystal at different temperatures. The dashed lines indicate the resonance voltages U_{res}.

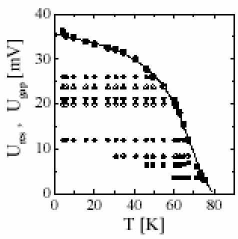

Ya.G.Ponomarev et al. Solid St.Commun. 111 (1999) 513

Conclusions-2

• **Intrinsic tunneling spectroscopy provides a unique way to probe BULK electronic properties of HTSC** (as opposed to surface tunneling spectroscopy, which is sensitive to surface deterioration at ~1 atomic layer, or formation of surface states)

Superconducting and Pseudo-gaps are clearly observed by intrinsic spectroscopy.

Temperature, Magnetic field and doping dependencies point towards different origins of the two gaps in HTSC.
(i) The pseudo-gap and the superconducting gap coexist at $T<Tc$. The PG does not continuously transform into the SG below Tc
(ii) Below Tc the PG hump position is correlated with the SG peak ⇒ convolution of two separate peaks in the DOS due to SIS tunneling.
(iii) Different T-dependencies: the SG vanishes at $T \to Tc$, while the PG is almost temperature independent.
(iv) Different H-dependencies: the SG vanishes at $H \to Hc2(T)$ and $Hc2(Tc) \to 0$; while the PG is almost field independent.
(v) Crossing of the SG and the PG at the doping phase diagram and indication for the existence of the critical doping point at p~0.19.

Possible applications of intrinsic Josephson junctions in cryo-electronics

Advantages:

- **Unique origin of all-HTSC tunnel junctions (due to very short coherence length and high chemical reactivity of HTSC)**
- **High quality junctions are pre-made by nature (~645 junctions/µm)**
- **Easy to integrate many junctions, perfect for 3D integration**
- **High T_c (Bi-2212 T_c=95K, Tl-2212 T_c=125K)**
- **High I_cR_n ~10-20 mV – High frequency applications (THz !)**

Possible applications:

- **Josephson volt standard** (prototype H.B.Wang, 2001)
- **Intrinsic SQUID** (demonstrated V.M.Krasnov, A.Irie, 2005)
- **Single electron transistor** (??? Yu. Latyshev, S-J.Kim 1999)
- **Flux-flow oscillators** (coherent, in-phase mode ???)
- **THz mixers/receivers**
- **Atomic scale multilayer devices** (Quantum Cascade Laser, …)
- **Magnetic flux transformers, Electric field transistors, etc…**

Prototype of the Josephson volt standard

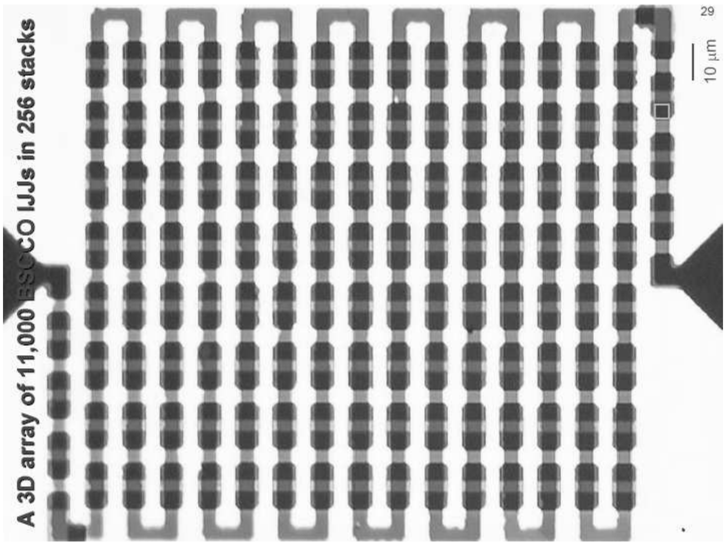

From: H.B.Wang et.al, Phys.Rev.Lett. 87 (2001) 107002

Intrinsic SQUID

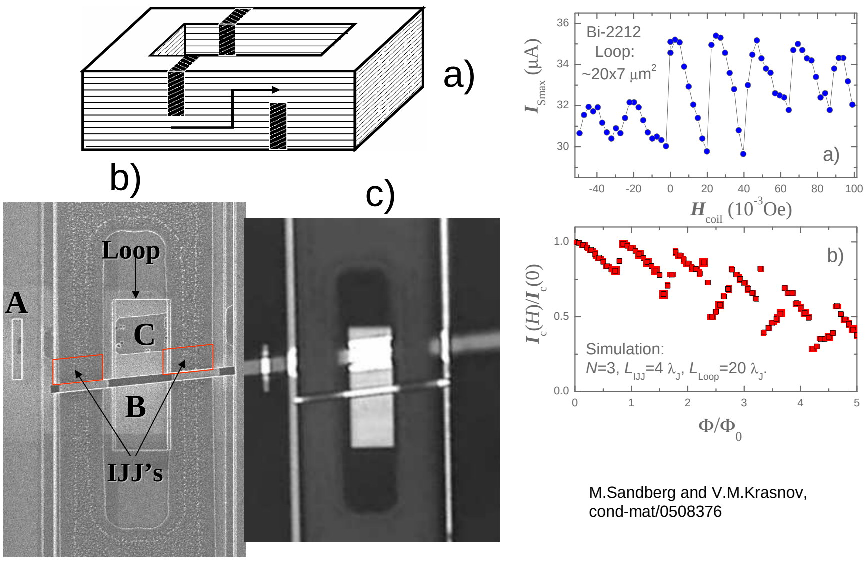

M.Sandberg and V.M.Krasnov, cond-mat/0508376

Intrinsic spin valve effect in layered manganite $La_{1.4}Sr_{1.6}Mn_2O_7$

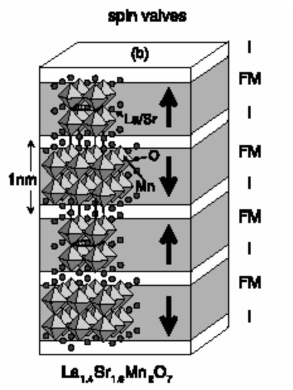

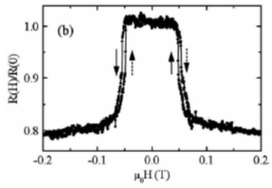

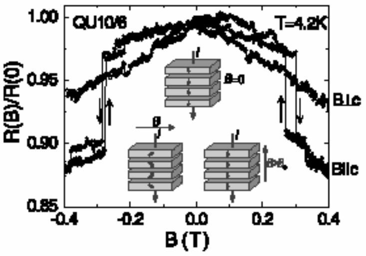

T. Nachtrab et al.,
Phys.Rev.B 65 (2001) 012410

Fig. 7. Magneto-resistance of LMSO mesa QU10/6 for field orientation parallel (solid symbols) and perpendicular (open symbols) to the layers. Bias current is set in the subgap regime of the *I–U* characteristic. Inset illustrates magnetization vectors for zero field, parallel field and perpendicular field above the threshold field where the jump in $R(B)$ occurs.

Interlayer tunneling spectroscopy of the charge density wave state in NbSe3

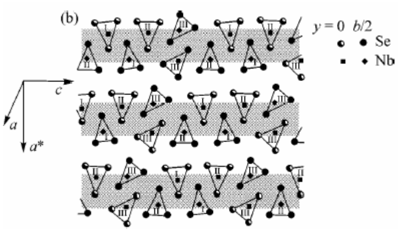

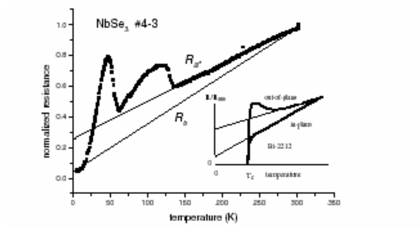

Figure 2. Normalized $R_{a^*}(T)/R_{a^*}(300)$ dependence for $NbSe_3$ stack #4-3. Straight lines show normalized metallic behaviour for the out-of-plane (R_{a^*}) and in-plane (R_b) dependences extrapolated to zero temperature. The insert schematically shows the similar difference of in-plane and out-of-plane metallic behaviour for Bi-2212.

Yu.I.Latyshev, et al., J.Phys.A 36 (2003) 9323

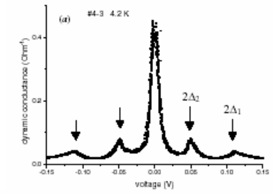

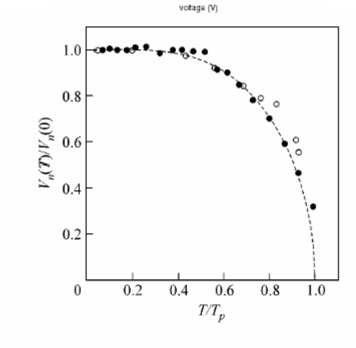

Fig. 5. Temperature dependence of the second Peierls energy gap for an overlap junction (sample No. 3, full circles) and a $NbSe_3$–$NbSe_3$ point contact (empty circles).

Conclusions: Natural atomic superlattices

• Natural atomic superlattices occur is a variety of strongly anisotropic layered compounds.
• Single crystals of such compounds represent stacks of atomic scale "Intrinsic" tunnel junctions

• Such materials often have unusual physical properties (charge/spin density waves, magnetism, high Tc superconductivity), related to low-dimensional electronic structure
• Intrinsic tunneling spectroscopy is a new powerful spectroscopic technique, which is indispensable for fundamental studies of bulk electronic properties of those materials

• Unique properties of intrinsic tunnel junctions can be used for electronic/spintronic applications at the ultimate atomic scale:

Advantages:

• Unique origin of tunnel junctions (HTSC)
• Highest quality – single crystals
• Pre-made by nature
• Easy to integrate many junctions, perfect for 3D integration
• Unique properties: High T_c, High I_cR_n, suitable for THz applications